JOC Article

Synthesis of Conformationally Constrained Peptidomimetics using Multicomponent Reactions

Rachel Scheffelaar,[†] Roel A. Klein Nijenhuis,[†] Monica Paravidino,[†] Martin Lutz,[‡] Anthony L. Spek,[‡] Andreas W. Ehlers,[†] Frans J. J. de Kanter,[†] Marinus B. Groen,[†] Romano V. A. Orru,*[,†] and Eelco Ruijter*[,†]

Department of Chemistry and Pharmaceutical Sciences, Vrije Universiteit Amsterdam, De Boelelaan 1083, 1081 HV Amsterdam, The Netherlands and Bijvoet Center for Biomolecular Research, Crystal and Structural Chemistry, Utrecht University, Padualaan 8, 3584 CH Utrecht, The Netherlands

orru@few.vu.nl; e.ruijter@few.vu.nl

Received September 17, 2008

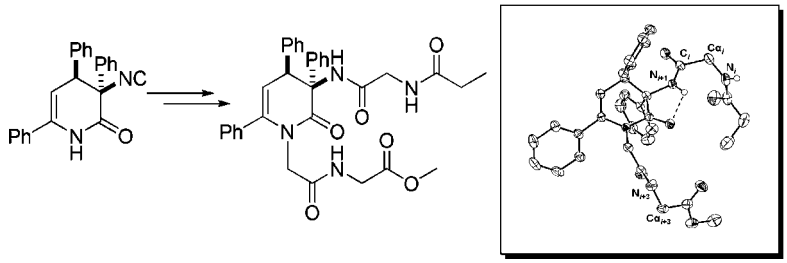

A novel modular synthetic approach toward constrained peptidomimetics is reported. The approach involves a highly efficient three-step sequence including two multicomponent reactions, thus allowing unprecedented diversification of both the peptide moieties and the turn-inducing scaffold. The turn-inducing properties of the dihydropyridone scaffold were evaluated by molecular modeling, X-ray crystallography, and NMR studies of a resulting peptidomimetic. Although modeling studies point toward a type IV β-turn-like structure, the X-ray crystal structure and NMR studies indicate an open turn structure.

Introduction

A major challenge in the field of peptidomimetics is the design and synthesis of conformationally constrained analogues that mimic secondary structural features of biologically active peptides or proteins. Among these structural motifs, the reverse turns commonly found in bioactive peptides are believed to be essential for protein folding.[1] Furthermore, they function as molecular recognition elements for the interaction between peptides and their receptors but also play an important role in antibody recognition.[2]

A well studied subset of the reverse turns are the β-turns (Figure 1A), which are defined as any tetrapeptide sequence occurring in the nonhelical region of a protein in which the $C\alpha_i - C\alpha_{i+3}$ spatial distance is ≤ 7 Å. In most cases, β-turns are stabilized by an intramolecular hydrogen bond between residues (i) and $(i + 3)$ forming a pseudo-10-membered ring.[1] Moreover, β-turns are classified according to the geometry of their peptide backbone, determined by the torsion angles φ and Ψ. Consequently, a range of different turn types (I−VIII) have been described.[1,3]

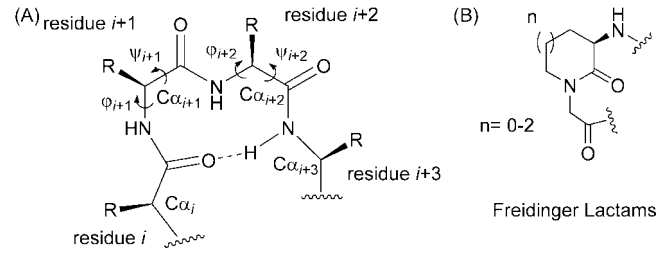

FIGURE 1. Schematic diagram of a β-turn (A) and the Freidinger lactams (B).

Topographical mimics of β-turns receive considerable attention in medicinal chemistry, and synthetic strategies for their preparation have evolved markedly in this area.[4] The incorpora-

[†] Vrije Universiteit Amsterdam.
[‡] Utrecht University.

(1) Rose, G. D.; Gierasch, L. M.; Smith, J. A. *Adv. Protein Chem.* **1985**, *37*, 1–109.
(2) Burgess, K. *Acc. Chem. Res.* **2001**, *34*, 826–835.
(3) (a) Venkatachalam, C. M. *Biopolymers* **1968**, *6*, 1425–1436. (b) Chou, P. Y.; Fasman, G. D. *J. Mol. Biol.* **1977**, *115*, 135–175. (c) Wilmot, C. M.; Thornton, J. M. *J. Mol. Biol.* **1988**, *203*, 221–232. (d) Ball, J. B.; Hughes, R. A.; Alewood, P. F.; Andrews, P. R. *Tetrahedron* **1993**, *49*, 3467–3478.

10.1021/jo802052j CCC: $40.75
Published on Web 12/04/2008

SCHEME 1. MCR toward 3,4-DHP-2-ones and Follow-Up Passerini Chemistry

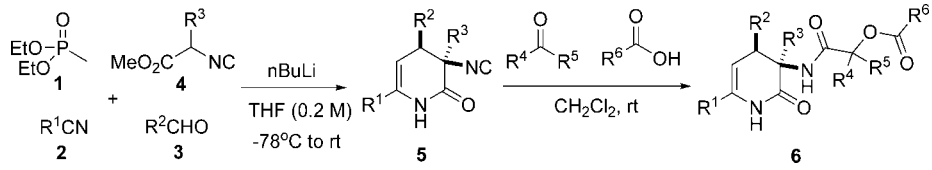

tion of conformational constraints can enhance the potency, receptor selectivity, and (peptidase) stability of the parent peptide.[4] Furthermore, it can provide useful information on the biologically active conformation of the peptide.[5] Among the various different strategies, of particular interest is the introduction of constrained dipeptide scaffolds, i.e., dipeptide isosters, in the parent peptide that are able to induce a folding of the peptide chain.[6] A pioneer in this field is Freidinger, who developed dipeptide γ-, δ-, ε-lactams (Figure 1B) as constrained scaffolds to stabilize turn conformations. He elegantly validated the concept by preparing a potent analogue of LHRH[7] (incorporation of a γ-lactam).[5,8]

In the course of a program directed toward the search for new multicomponent methodologies to access pharmaceutically relevant heterocyclic scaffolds,[9] we recently developed a novel four-component reaction (4CR) of phosphonate **1**, nitriles **2**, aldehydes **3**, and α-aryl isocyanoacetates **4** to obtain 3,4-dihydropyridin-2-ones **5** (3,4-DHP-2-ones). This 4CR generally proceeds in good to excellent yields and with complete diastereoselectivity in favor of the *cis*-diastereomer.[10] The 4CR is highly chemoselective, leaving the rather reactive isonitrile functionality intact. This exceptional chemoselectivity allows isonitrile-based follow-up chemistry. This was demonstrated by

SCHEME 2. Retrosynthetic Analysis of MCR-Derived Constrained Peptidomimetics

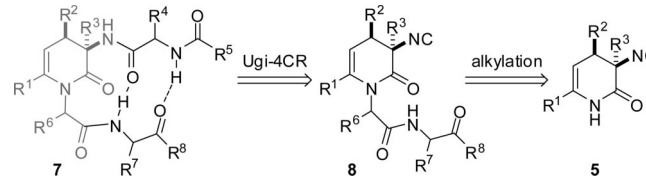

performing a Passerini 3CR to construct highly functionalized and conformationally constrained depsipeptides **6** in a novel 6CR (Scheme 1).[11] The structural resemblance of the DHP-2-one scaffold in **5** to the Freidinger lactams inspired us to investigate its potential as a turn-inducing moiety. Our strategy involves a modular MCR−alkylation−MCR sequence. After the initial 4CR to access the DHP-2-one scaffold as the Freidinger-type lactam, construction of the dipeptide isoster (given in gray, Scheme 2) can be realized by introduction of a peptide chain onto the DHP-2-one core by N-alkylation. After this a second MCR, e.g., a Passerini 3CR or Ugi 4CR (Scheme 2), is envisioned. This introduces a second (depsi)peptide chain. In case of an Ugi-4CR this would complete a tetrapeptide (or larger) sequence, in which the turn conformation can in principle be stabilized by two intramolecular hydrogen bonds. Most synthetic methods for Freidinger-type lactams lack flexibility and are therefore not suited to introduce diversity.[12] This is, however, important because the lactam ring is often positioned in the pharmacophoric region of the peptide. Flexible synthetic methodology toward Freidinger-type lactams and the corresponding tetrapeptide turn-mimics are of considerable interest to facilitate optimization studies.[12] Our 4CR for the synthesis of the DHP-2-one core is very flexible, and variation of all components proved possible.[10] In addition, the modular MCR−alkylation−MCR strategy as discussed above further increases the number of diversity points, making our approach ideally suited for the generation of libraries of conformationally constrained peptidomimetics and potential β-turn mimetics.[13] In this paper we discuss the results of our synthetic studies and the turn-inducing properties of the resulting peptidomimetics in full detail.

Results and Discussion

Modeling Studies. Hydrophobic and in particular aromatic elements in receptor ligands often play an important role in recognition and activation of receptors possessing lipophilic domains, and that is why many ligand mimics contain these lipophilic elements.[14] Numerous effective benzo-fused Freidinger lactams and benzodiazepine mimics (mostly antagonists)

(4) For reviews on peptidomimetics, see: (a) Ball, J. B.; Alewood, P. F. *J. Mol. Recognit.* **1990**, *3*, 55–64. (b) Giannis, A.; Kolter, T. *Angew. Chem., Int. Ed. Engl.* **1993**, *32*, 1244–1267. (c) Gante, J. *Angew. Chem., Int. Ed. Engl.* **1994**, *33*, 1699–1720. (d) Hanessian, S.; McNaughton-Smith, G.; Lombart, H.-G.; Lubell, W. D. *Tetrahedron* **1997**, *53*, 12789–12854. (e) Giannis, A.; Rübsam, F. *Advances in Drug Research*; Test, B., Ed.; Academic Press: London, 1997; Vol. 29, pp 1−78. (f) Synthesis of Peptides and Peptidomimetics. In *Houben-Weyl, Methods of Organic Chemistry*; Felix, A., Moroder, L., Toniolo, C., Eds.; Thieme: Stuttgart, New York, 2003; Vol. E22c. (g) Kee, S.; Jois, S. D. S. *Curr. Pharm. Des.* **2003**, *9*, 1209–1224. (h) Perdih, A.; Kikelj, D. *Curr. Med. Chem.* **2006**, *13*, 1525–1556.

(5) A good illustration of this concept is the constrained analogue of LHRH (see ref 7) by Freidinger: Freidinger, R. M.; Veber, D. F.; Perlow, D. S.; Brooke, J. R.; Saperstein, R. *Science* **1980**, *210*, 656–658.

(6) See also ref 4. For recent examples, see: (a) Palomo, C.; Aizpurua, J. M.; Benito, A.; Miranda, J. I.; Fratila, R. M.; Matute, C.; Domercq, M.; Gago, F.; Martin-Santamaria, S.; Linden, A. *J. Am. Chem. Soc.* **2003**, *125*, 16243–16260. (b) Ecija, M.; Diez, A.; Rubiralta, M.; Casamitjana, N. *J. Org. Chem.* **2003**, *68*, 9541–9553. (c) Dietrich, S. A.; Banfi, L.; Basso, A.; Damonte, G.; Guanti, G.; Riva, R. *Org. Biomol. Chem.* **2005**, *3*, 97–106. (d) Van Rompaey, K.; Ballet, S.; Tömböly, C.; De Wachter, R.; Vanommeslaeghe, K.; Biesemans, M.; Willem, R.; Tourwé, D. *Eur. J. Org. Chem.* **2006**, 2899–2911. (e) Einsiedel, J.; Lanig, H.; Waibel, R.; Gmeiner, P. *J. Org. Chem.* **2007**, *72*, 9102–9113.

(7) LHRH: luteinizing hormone-releasing hormone.

(8) (a) Freidinger, R. M.; Veber, D. F.; Hirschmann, R.; Paege, L. M. *Int. J. Pept. Protein Res.* **1980**, *16*, 464–470. (b) Freidinger, R. M.; Perlow, D. S.; Veber, D. F. *J. Org. Chem.* **1982**, *47*, 104–109. (c) Freidinger, R. M. *J. Med. Chem.* **2003**, *46*, 5553–5566.

(9) (a) Bon, R. S.; Van Vliet, B.; Sprenkels, N. E.; Schmitz, R. F.; de Kanter, F. J. J.; Stevens, C. V.; Swart, M.; Bickelhaupt, F. M.; Groen, M. B.; Orru, R. V. A. *J. Org. Chem.* **2005**, *70*, 3542–3553. (b) Vugts, D. J.; Koningstein, M. M.; Schmitz, R. F.; de Kanter, F. J. J.; Groen, M. B.; Orru, R. V. A. *Chem. Eur. J.* **2006**, *12*, 7178–7189. (c) Elders, N.; Schmitz, R. F.; de Kanter, F. J. J.; Ruijter, E.; Groen, M. B.; Orru, R. V. A. *J. Org. Chem.* **2007**, *72*, 6135–6142. (d) Groenendaal, B.; Vugts, D. J.; Schmitz, R. F.; de Kanter, F. J. J.; Ruijter, E.; Groen, M. B.; Orru, R. V. A. *J. Org. Chem.* **2008**, *73*, 719–722. (e) Elders, N.; de Kanter, F. J. J.; Ruijter, E.; Groen, M. B.; Orru, R. V. A. *Chem. Eur. J.* **2008**, *14*, 4961–4974. (f) Groenendaal, B.; Ruijter, E.; de Kanter, F. J. J.; Lutz, M.; Spek, A. L.; Orru, R. V. A. *Org. Biomol. Chem.* **2008**, *6*, 3158–3165.

(10) Paravidino, M.; Bon, R. S.; Scheffelaar, R.; Vugts, D. J.; Znabet, A.; Schmitz, R. F.; de Kanter, F. J. J.; Lutz, M.; Spek, A. L.; Groen, M. B.; Orru, R. V. A. *Org. Lett.* **2006**, *8*, 5369–5372.

(11) Paravidino, M.; Scheffelaar, R.; Schmitz, R. F.; de Kanter, F. J. J.; Groen, M. B.; Ruijter, E.; Orru, R. V. A. *J. Org. Chem.* **2007**, *72*, 10239–10242.

(12) Golebiowski, A.; Jozwik, J.; Klopfenstein, S. R.; Colson, A.-O.; Grieb, A. L.; Russell, A. F.; Rastogi, V. L.; Diven, C. F.; Portlock, D. E.; Chen, J. J. *J. Comb. Chem.* **2002**, *4*, 584–590.

(13) For a review on β-turn mimetic library synthesis, see: Souers, A. J.; Ellman, J. A. *Tetrahedron* **2001**, *57*, 7431–7448.

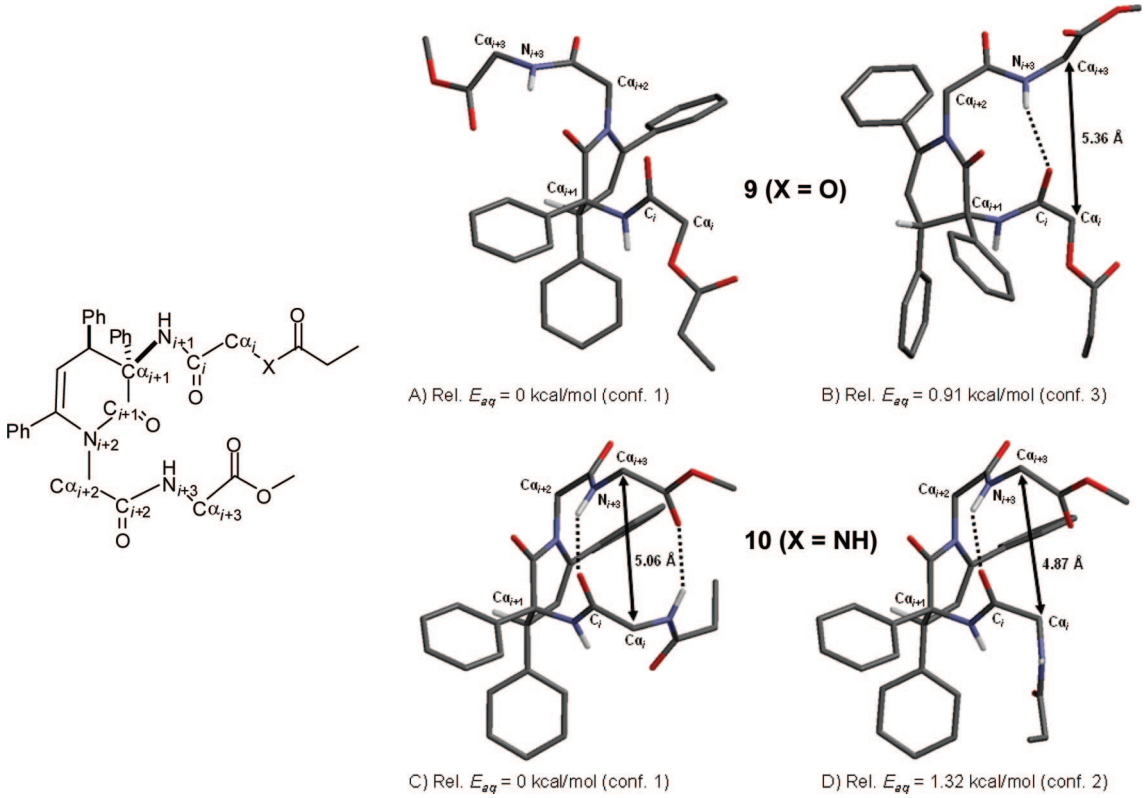

FIGURE 2. Representation of the lowest energy conformers of model systems **9** and **10**.

TABLE 1. Two Lowest Energy Conformers of 9 and 10 Adopting a β-Turn Geometry and Calculated Values of the Different Geometrical Parameters

	$d(C\alpha_i - C\alpha_{i+3})$ [Å]	$d(CO_i - NH_{i+3})$ [Å]	φ_{i+1}[a] [deg]	Ψ_{i+1}[b] [deg]	φ_{i+2}[c] [deg]	Ψ_{i+2}[d] [deg]	E_{aq} (kcal/mol)	β-turn type
9 (conformer 1)	8.87	4.75	28	77	−86	67	−176.14	
9 (conformer 3)	5.36	2.36	45	73	84	−58	−175.23	IV
10 (conformer 1)	5.06	2.15	49	73	84	−45	−136.72	IV
10 (conformer 2)	4.87	2.14	34	71	87	−48	−135.40	IV

[a] φ_{i+1} = torsion angle $C_i - N_{i+1} - C\alpha_{i+1} - C_{i+1}$. [b] Ψ_{i+1} = torsion angle $N_{i+1} - C\alpha_{i+1} - C_{i+1} - N_{i+2}$. [c] φ_{i+2} = torsion angle $C_{i+1} - N_{i+2} - C\alpha_{i+2} - C_{i+2}$. [d] Ψ_{i+2} = torsion angle $N_{i+2} - C\alpha_{i+2} - C_{i+2} - N_{i+3}$.

have been reported.[4h] Therefore, we chose, the DHP-2-one scaffold **5a** ($R^1 = R^2 = R^3 =$ Ph) as the standard heterocyclic core and potential turn-inducing element in model systems **9** and **10**. After the 4CR to access **5a**, depsipeptide **9** and amide variant **10** can, in principle, be prepared by combining an alkylation with the Passerini 3CR and Ugi 4CR, respectively, as outlined above. However, to determine the propensity of the 3,4-DHP-2-one scaffold to indeed induce a β-turn-like conformation in **9** and **10**, modeling studies using Spartan 02 were performed first (Figure 2). The procedure consists of a MM-SYBYL conformational search followed by an AM1 geometry optimization and single point energy calculation using AM1 including solvent effects (SM5). The turn-inducing propensity of the lowest energy conformers of **9** and **10** was evaluated by analyzing different geometrical features: (1) the $C\alpha_i - C\alpha_{i+3}$ distance (d) (<7 Å); (2) the φ and Ψ backbone torsion angles in residues 2 and 3; (3) the distance between the carbonyl oxygen of residue 1 and the amide proton of residue 4 indicative for intramolecular hydrogen bonding (<2.5 Å).

The lowest energy conformer of depsipeptide **9** has a linear conformation and is therefore not a β-turn (Figure 2A). The lowest energy conformer that adopts a turn conformation (type IV, the third conformation, Figure 2B) is 0.91 kcal/mol above the global minimum. Considering the error margins of the method used, this is a feasible conformation. In contrast, the lowest energy conformer of tetrapeptide **10** shows to be a β-turn of type IV according to the backbone torsion angle classification (Table 1 and Figure 2C). In addition to a turn-stabilizing hydrogen bond forming a pseudo-10-membered ring, a second stabilizing intramolecular hydrogen bond is present in conformer 2C of tetrapeptide **10**, forming a pseudo-14-membered ring. The second lowest energy conformer (1.32 kcal/mol above the global minimum, Figure 2D) is also a type IV turn, although it lacks the second intramolecular hydrogen bond. Moreover, within 4.0 kcal/mol several more turn structures were found. Thus, the tetrapeptide model system **10** has a higher probability (potential) to indeed adopt a turn conformation.

Synthesis. After these promising results, we decided to study the follow-up Ugi 4CR on the 3,4-DHP-2-one scaffold. In principle, Freidinger lactam-like structures as **10** are available from MCR product **5a** ($R^1 = R^2 = R^3 =$ Ph) by two possible synthetic routes, i.e., Ugi 4CR followed by N1-alkylation or N1-alkylation followed by Ugi 4CR. Since reaction of **5a** with

(14) (a) Marshall, G. R. *Curr. Opin. Struct. Biol.* **1992**, *2*, 904–919. (b) Giannis, A.; Kolter, T. *Angew. Chem., Int. Ed. Engl.* **1993**, *32*, 1244–1267.

TABLE 2. Alkylation of the DHP-2-one 5a and Ugi Follow-Up Chemistry on Alkylated DHP-2-one 11

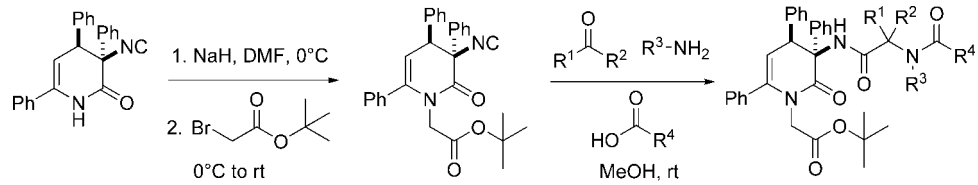

5a **11** 93% **12**

Entry	R^1	R^2	R^3	R^4	Ugi Product	Reaction time (h)	Yield (%)[b]
1	H	H	Bn	Et	**12a**	22	100
2	H	H	Bn	Ph	**12b**	22	86
3	H	H	Bn		**12c**	22	91
4	H	H	DMB	Et	**12d**	28	55
5	H	H	DMB		**12e**	6	45
6	H	H	nBu	Et	**12f**	24	86
7[c]	iPr	H	Bn	Et	**12g**	18	95
8[c]	Ph	H	Bn	Et	**12h**	50	59
9	H	H	Ph	Et	**12i**	114	32[d]
10[c]	iPr	H	Ph	Et	**12j**	16	59[e]
11	Me	Me	Bn	Et	**12k**	165	77

[a] Unless otherwise noted (see Supporting Information), the Ugi 4CRs were carried out using 0.88 M of DHP-2-one **11** with 1.1 equiv of carboxylic acid and 1.5 equiv of both aldehyde and amine [b] Isolated yields are reported. [c] A 1:1 mixture of diastereomers was obtained. [d] Along with the product also 45% of side product **15** was isolated. [e] Along with the product also 23% of side product **14** was isolated. DMB = dimethoxybenzyl.

isobutyraldehyde, benzylamine and propionic acid did not afford the expected Ugi product, the former route was abandoned. On the other hand, **5a** could be alkylated with *tert*-butyl bromoacetate after deprotonation with NaH in excellent yield (93%) to give **11** (Table 2). To our delight, the Ugi 4CR involving **11**, isobutyraldehyde, benzylamine, and propionic acid indeed succeeded, affording the Ugi product **12g** in nearly quantitative yield (Entry 7, Table 2). To determine the generality of this approach, the scope of the Ugi reaction was studied in more detail. Isocyanide **11** was reacted with several commercially available aldehydes, amines, and acids under standard Ugi conditions (MeOH, rt). In this study, the DHP-2-one starting material **11** ($R^1 = R^2 = R^3 =$ Ph) was not varied as we have shown this extensively in our previous work.[10,11]

The expected Ugi products **12a**−**k** were obtained in moderate to excellent yields (32−100%) with reaction times varying from 6 h to 7 days (Table 2). When aldehydes other than paraformaldehyde were applied, approximately 1:1 mixtures of diastereomers were obtained. The diastereomers could only be separated for the example applying benzaldehyde (**12h**, entry 8, Table 2). Table 2 shows the broad substrate scope of the reaction, and no limitations were found in any of the components. When paraformaldehyde and aniline (entry 9, Table 2) were used as components, a lower yield was obtained as a result of the formation of an iminoimidazolidine side product **15** (45%, Scheme 3). Ugi reactions involving aniline in combination with formaldehyde (or paraformaldehyde) are rare and afford the desired product in moderate yield at best.[15] The initial products of the reaction between formaldehyde and aromatic amines are carbinolamines,[16] which will react further to the Ugi product most likely via an imine or iminium ion intermediate.[17] Imine formation between (para)formaldehyde and aniline is expected to be a slow process compared to the formation of other imines due to the limited nucleophilic character of aniline and the rather high stability of the carbinolamine.[16] This also explains the long reaction time of this particular Ugi reaction and the formation of side products such as the iminoimidazolidine **15**. The formation of **15** is most likely caused by relatively high concentration of free aniline during the reaction, resulting from slow imine formation and the rather low basicity of aniline.

(15) (a) Umkehrer, M.; Kalinski, C.; Kolb, J.; Burdack, C. *Tetrahedron Lett.* **2006**, *47*, 733–737. (b) Kalinski, C.; Umkehrer, M.; Ross, G.; Kolb, J.; Burdack, C.; Hiller, W. *Tetrahedron Lett.* **2006**, *47*, 2391–2393. (c) Maison, W.; Schlemminger, I.; Westerhoff, O.; Martens, J. *Bioorg. Med. Chem.* **2000**, *8*, 1343–1360.

(16) (a) Abrams, W. R.; Kallen, R. G. *J. Am. Chem. Soc.* **1976**, *98*, 7777–7789. (b) Atherton, J. H.; Brown, K. H.; Crampton, M. R. *J. Chem. Soc., Perkin Trans. 2* **2000**, 941–946. The rather high stability of the carbinolamine and therefore slow formation of the imine most likely explains the long reaction time of this particular Ugi reaction and the formation of side products such as the iminoimidazolidine.

(17) There is evidence that pure *N*-methyleneaniline occurs as a cyclic trimer. However, since nucleophilic species are present the formation of this trimer is not likely. See: Miller, J. G.; Wagner, E. C. *J. Am. Chem. Soc.* **1932**, *54*, 3698–3706.

SCHEME 3. Formation of α-Amino Amidine and Iminoimidazolidine Side Products Using Aniline in the Ugi Reaction of 11

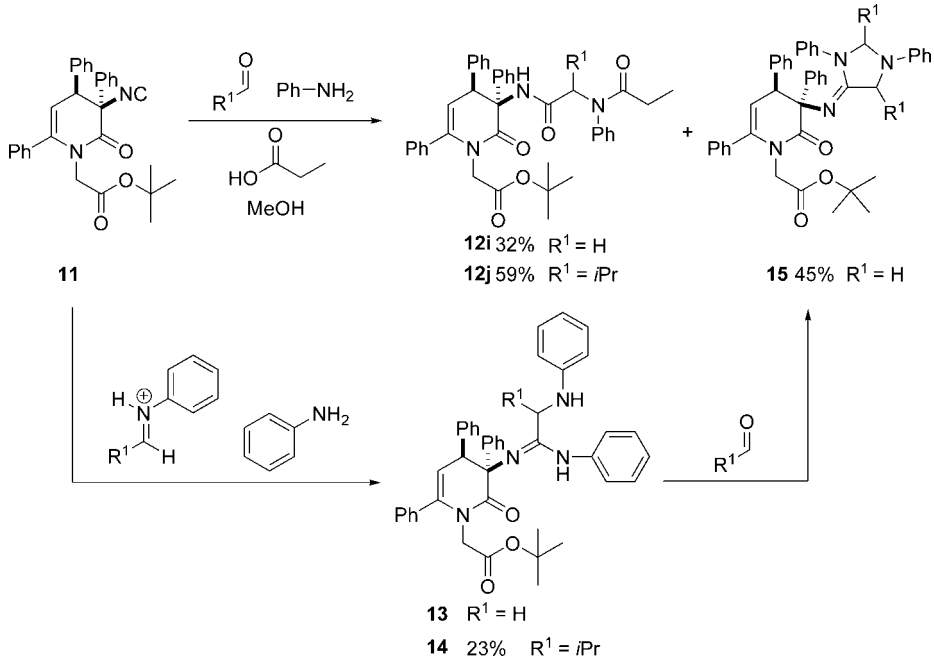

SCHEME 4. Synthetic Route toward Model Structures 9 and 10

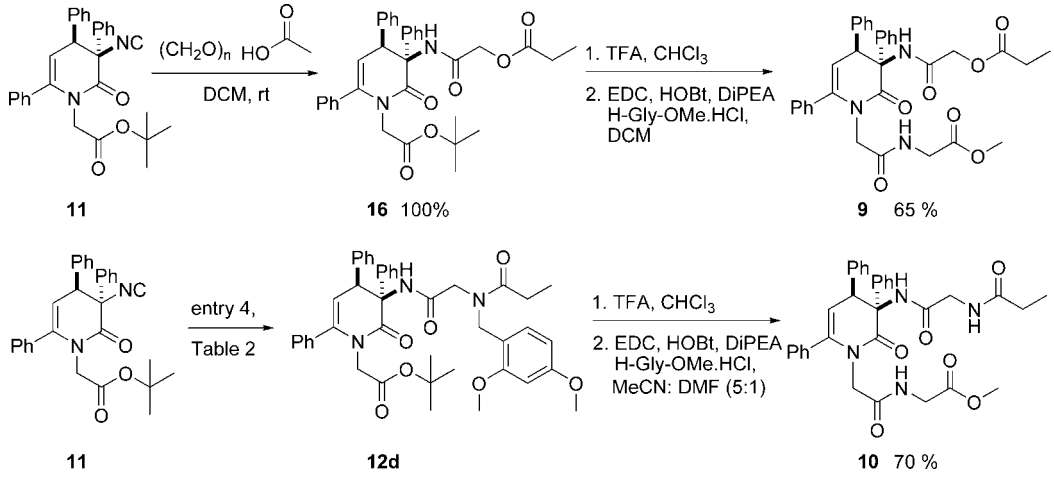

The higher nucleophilicity of aniline compared to the carboxylate anion then results in the intermediate α-amino amidine **13** rather than the Ugi product **12i**.[18] Since paraformaldehyde is quite unhindered, a subsequent ring closure is possible by reaction of intermediate **13** with a second equivalent of (para)formaldehyde to give **15**. The formation of α-amino amidines via this Ugi-type condensation has been reported earlier by McFarland, who needed 1 equiv of dimethylamine hydrochloride to facilitate the reaction.[19] Later, Keung et al. optimized this procedure by replacing the stoichiometric ammonium salt by a catalytic amount of scandium triflate.[20] The presence of acid and free amine in the reaction above (entry 9, Table 2) can account for observation of this side reaction.

When isobutyraldehyde, aniline, and propionic acid were employed in the Ugi reaction, a higher yield of Ugi product **12j** was obtained (58%), albeit accompanied by α-amino amidine **14** (23%). In this case, cyclization to the corresponding iminoimidazolidine product was not observed, most likely because isobutyraldehyde is too sterically hindered. In conclusion, in the majority of combinations that were tested the Ugi reaction can be performed successfully after alkylation of the DHP-2-one scaffold **5a**.

To investigate the actual turn-inducing capacities of the DHP-2-one scaffold, model structures **9** and **10** were synthesized (Scheme 4) using the MCR−alkylation−MCR sequence. Thus after initial 4CR and alkylation, chemoselective condensation of the isocyano function in DHP-2-one **11** using a Passerini 3CR reaction with paraformaldehyde and propionic acid gave **16** in quantitative yield. *tert*-Butyl deprotection and subsequent EDC/HOBt-mediated coupling proceeded smoothly in 65% overall yield to afford constrained depsipeptide **9**. A similar strategy employing a 4CR-alkylation-Ugi 4CR sequence gave

(18) The formation of this intermediate could be proven by stirring **11** with paraformaldehyde (3 equiv) and aniline (3 equiv) to give 45% of **15** and 10% of amidine **13** (reaction time 77) h). When 1.0 equiv of Et_3N·HCl was added, the amidine was not present after 77 h and the yield of **15** is 73%. During the reaction, however, **13** was observed on TLC, supporting its involvement as an intermediate.

(19) McFarland, J. W. *J. Org. Chem.* **1963**, *28*, 2179–2181.

(20) Keung, W.; Bakir, F.; Patron, A. P.; Rogers, D.; Priest, C. D.; Darmohusodo, V. *Tetrahedron Lett.* **2004**, *45*, 733–737.

SCHEME 5. Synthesis of Pentapeptide Mimics 19a−d

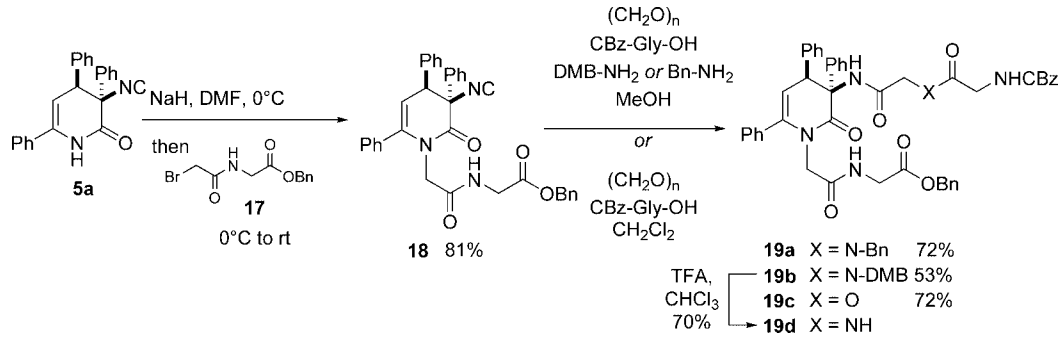

the Ugi product **12d** (entry 4, Table 2), which was subsequently subjected to *tert*-butyl deprotection and subsequent EDC/HOBt-mediated coupling to obtain the corresponding tetrapeptide mimic **10**. The DMB group was removed simultaneously with the *tert*-butyl group under acidic conditions. A different solvent system was required (MeCN/DMF 5:1 instead of CH_2Cl_2) to dissolve the free acid for the coupling reaction to allow the isolation of **10** in 70% yield.

Our modular MCR−alkylation−MCR strategy can also be used to directly attach peptide moieties to both positions of the DHP-2-one scaffold. This further improves the flexibility, ease of handling, and general applicability of our method to arrive at potential turn mimics based on Freidinger-type lactams. Thus, alkylation of **5a** with $BrCH_2C(O)$-Gly-OBn (**17**) cleanly gave isocyanide **18**, which could be used in subsequent Ugi or Passerini reactions to give constrained pentapeptides **19a** and **19b** and depsipeptide **19c** (Scheme 5). The DMB group in **19b** could then be cleaved by treatment with TFA to give **19d** in 70% yield.

Conformational Analysis. The results from the computational modeling studies showed that the DHP-2-one core in both the depsipeptide **9** and the tetrapeptide **10** indeed could serve as a turn-inducing element and that for both model systems a β-turn (type IV) is a viable conformation. With **9** and the **10** in hand we now decided to undertake a detailed spectroscopic study on the secondary structure of these model systems.

X-ray Crystal Structure Determination. We were able to produce crystals of the tetrapeptide **10** that were of sufficient quality for a detailed X-ray diffraction. Figure 3 shows the molecular structure of **10** in the crystal, clearly adopting a turn conformation. However, no intramolecular hydrogen bond is present between CO_i and NH_{i+3}. Instead, there is an intramolecular hydrogen bond between N_{i+1} and CO_{i+1} and the other two amide protons (NH_i and NH_{i+3}) participate in a one-dimensional chain in the direction of the crystallographic *a*-axis by intermolecular hydrogen bonds. The presence of the intramolecular hydrogen bond between N_{i+1} and CO_{i+1} excludes the possibility of an intramolecular hydrogen bond between CO_i and NH_{i+3}. The peptide chains are rotated to such an extent that the interstrand distance becomes to long for hydrogen bonding contacts. An important criterion for β-turns is that the $C\alpha_i-C\alpha_{i+3}$ distance should be smaller than 7 Å. The X-ray crystal structure shows a $C\alpha_i-C\alpha_{i+3}$ distance of 8.949(2) Å, and although **10** clearly adopts a turn structure, it can not be classified as a β-turn.

To compare these results to the modeling results on the conformation of **10** described above, the energy (E_{aq}) of the conformation in the X-ray crystal structure was calculated using the same geometry optimization//AM1-SM5 single point energy calculations. This E_{aq} appeared to be −132.3 kcal/mol, which is 4.4 kcal/mol above the modeled lowest energy conformer (E_{aq} = −136.72 kcal/mol, see also Table 1) of **10**.

The two somewhat contradictory results of the modeling studies and the X-ray crystal structure can be rationalized by the different media in which the experiments are performed. The modeling experiments deal with gas phase conformations and therefore intermolecular interactions are not taken into account. On the other hand, in the X-ray crystal structure packing forces become important, which is of course facilitated by intermolecular hydrogen bonds and which may lead to a change in secondary structure. Intermolecular forces are of primary importance in crystal formation.[21] Both methods by definition do not give the correct representation of the secondary conformation of **10** in solution, so further solution phase studies by NMR (low concentration) were required.

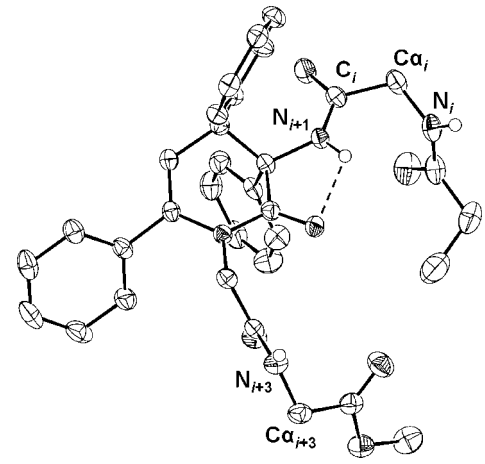

FIGURE 3. Displacement ellipsoid plot of **10**. Drawn at 50% probability level. The compound was crystallized from a benzene/CH_2Cl_2 mixture (1:1) by slow evaporation as a racemate in the centrosymmetric space group $P2_1/c$. Only N−H hydrogen atoms of the amide groups are drawn, for clarity. $d(C\alpha_i-C\alpha_{i+3})$ = 8.949(2) Å; torsion angles with standard uncertainties: φ_{i+1} = 175.75(14)°, Ψ_{i+1} = 167.27(12)°, φ_{i+2} = −68.44(16)°, Ψ_{i+2} = 159.23(12)°; E_{aq}= −132.3 kcal/mol.

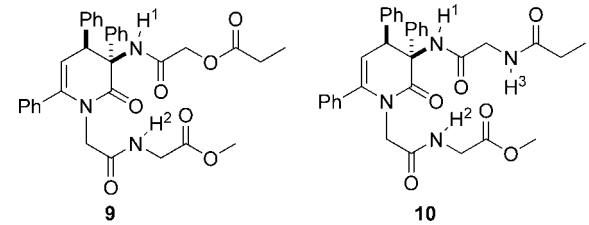

FIGURE 4. Model compounds **9** and **10** used for the conformational analysis including amide proton numbering.

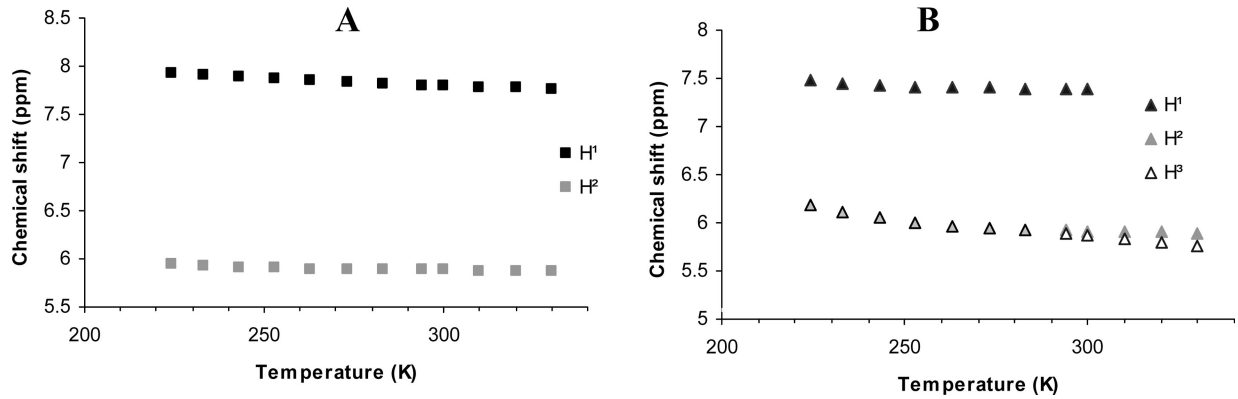

FIGURE 5. Chemical shift values at different temperatures for the different amide protons of model compounds **9** (A) and **10** (B).

TABLE 3. Chemical Shifts in $CDCl_3$, Solvent Effect (in Brackets), and Temperature Coefficients of Amide Protons in 9 and 10[a]

compd	δH^1 (ppm)	δH^2 (ppm)	δH^3 (ppm)	$\Delta\delta H^1/\Delta T$ (ppb/K)[b]	$\Delta\delta H^2/\Delta T$ (ppb/K)[b]	$\Delta\delta H^3/\Delta T$ (ppb/K)[b]
9	7.80 (0.14)	5.88 (2.34)		−2.22 to −0.98[c]	−1.21 to −0.42[c]	
10	7.39 (0.49)	5.92 (2.32)	5.86 (2.16)	−2.38 to −0.05[d]	−0.94 to −0.53[e]	−3.57 to −2.88[e]

[a] All NMR experiments were performed using 1.0−2.0 mM $CDCl_3$ solutions; chemical shift values (δ) reported are the values at 300 K. Data in brackets correspond to δ(DMSO) − δ($CDCl_3$) (ppm, 300 K). [b] Temperature coefficients were determined between all successive data points; highest and lowest values are reported. [c] Temperature coefficients were determined between 233 and 330 K. [d] Temperature coefficient were determined between 233 and 300 K. [e] Temperature coefficient were determined between 294 and 330 K.

^{1}H NMR Studies. The conformational behavior of model structures **9** and **10** (Figure 4) in solution was also investigated using 1-D and 2-D NMR techniques.

Full assignment of the different methylene and the amide NH protons was achieved using gs-HMBC and gs-NOESY NMR measurements. 2D ^{1}H NOESY NMR data did not suggest the close proximity of the two peptide chains, since no interstrand correlations, but only intrastrand contacts, were observed.

The presence of intramolecular hydrogen bonding was determined by evaluation of the chemical shift values of the amide NH protons and their temperature coefficients ($\Delta\delta$H/ΔT). Hydrogen-bonded amide protons have a high chemical shift value ($\delta \geq 7.0$ ppm) and display a very small temperature coefficient (0 to −3.0 ppb/K). Non-hydrogen-bonded protons usually show a low chemical shift value ($\delta \leq 7.0$ ppm) and also a very small temperature coefficient (0 to −3.0 ppb/K). Large temperature coefficients (between −4 and −8 ppb/K) indicate equilibrium between hydrogen-bonded and non-hydrogen-bonded states.[22]

Figure 5 shows the temperature dependence of the chemical shifts of the amide protons of **9** and **10**. Spectra were recorded from 224 to 330 K with increments of approximately 10 K using 1−2 mM solutions in $CDCl_3$ to avoid intermolecular interactions.[23] The chemical shift values of the H^1 amide protons of both compounds appear downfield ($\delta > 7.0$ ppm), which is an indication of hydrogen bonding. On the other hand, amide protons H^2 of both compounds and H^3 of **10** appear upfield ($\delta < 6.0$ ppm), indicative for a non-hydrogen-bonded state.

Table 3 shows the chemical shifts (ppm) values at 300 K and temperature coefficients (ppb/K) for the amide NH protons of **9** and **10**. Temperature coefficients were determined between all successive data points (highest and lowest values are reported in Table 3).[24,25]

The temperature coefficient for H^1 of both compounds is very small (<3 ppb/K, in absolute value), which supports (together with the high chemical shift values) a hydrogen bonded state.

For compound **10**, signals for H^2 and H^3 overlap significantly in the 233−283 K range. Accordingly, temperature coefficients could be most accurately determined for the 294−330 K range, and these values are reported in Table 3.[26] The coefficient for H^2 of both compounds is small, but since the chemical shift value is below 6.0 ppm this indicates a non-hydrogen-bonded state. The H^3 amide proton of **10** has a slightly higher temperature coefficient (average of −3 ppb/K), which may indicate a small amount of hydrogen bonding. However, considering the chemical shift value of this proton, this is most likely very small and negligible.

A third indication of intramolecular hydrogen bonding is the effect on the chemical shift upon switching from the non-hydrogen-bonding solvent $CDCl_3$ to the hydrogen-bond-acceptor solvent DMSO. Strongly hydrogen-bonded amide protons are not accessible to the solvent and have a small chemical shift difference ($\Delta\delta < 0.2$ ppm in absolute value). Non-hydrogen-bonded amide protons are accessible to the solvent and have a large chemical shift difference ($\Delta\delta > 0.2$ ppm in absolute value, usually larger than 1.0 ppm).[24] The solvent effect on the chemical shifts of protons H^1, H^2, and H^3 of compounds **9** and **10** are given in brackets (Table 3).[24] The chemical shift difference of H^1 in **9** is small ($\Delta\delta = 0.14$ ppm in absolute value) when the solvent is changed to DMSO, but a large chemical shift difference is observed for H^2 ($\Delta\delta = 2.34$ ppm) indicating

(21) See ref 6a and references therein.
(22) Belvisi, L.; Gennari, C.; Mielgo, A.; Potenza, D.; Scolastico, C. *Eur. J. Org. Chem.* **1999**, 389–400.
(23) Boussard, G.; Marraud, M. *J. Am. Chem. Soc.* **1985**, *107*, 1825–1828.
(24) For all data, see Supporting Information.
(25) In general, the coefficients have the largest values at lower temperatures and become more or less constant at room temperature, which can be explained by an increased amount of intermolecular hydrogen bonding at lower temperatures. Specifically high coefficients are found in the 224−233 K interval, accompanied with line broadening of the ^{1}H NMR signals (especially for **10**). These values are therefore not reliable and were excluded from the table.
(26) Although the signals for H2 and H3 overlap in the 233−283 K range, it is clear from Figure 5B that the temperature coefficients for both protons are significantly larger than in the 294−330 K range. However, it must be noted that high temperature coefficients are especially observed in the low temperature range, where line broadening (possibly due to aggregation) is observed.

a non-hydrogen-bonded situation. Amide proton H^1 of the Ugi derivative **10** has a slightly higher solvent coefficient ($\Delta\delta$ = 0.49 ppm in absolute value) indicating that this proton is accessible to the solvent. Moreover, both amide protons H^2 and H^3 have very large solvent coefficients and are therefore clearly non-hydrogen-bonded. According to the chemical shift value and temperature coefficient experiments H^1 was locked in a hydrogen bonded conformation (in $CDCl_3$). However, apparently pure DMSO is a too strong competitive hydrogen bond acceptor. DMSO titration studies in $CDCl_3$ indicated that the chemical shift of H^1 in **10** is constant up to 20% of DMSO and can therefore be considered as hydrogen-bonded.[24] All of the ^1H experiments described above indicate that amide protons H^1 of both model compounds **9** and **10** are involved in intramolecular hydrogen bonds. However, no intramolecular hydrogen bond is present between the two peptide chains. This is in agreement with the X-ray crystal structure and therefore these Freidinger-type peptidomimetics most likely do not fulfill the criteria of a β-turn. In fact, the various NMR studies all suggest a conformation very similar to that in the X-ray crystal structure.

Conclusion

Although the MM-SYBYL-AM1 analysis indicated realistic type IV β-turn conformations for our model systems, the spectroscopic data only confirm that the DHP-2-one scaffold does induce a turn, albeit not a true β-turn conformation. However, the rigidification introduced by the ring, the presence of the intramolecular hydrogen bond between N_{i+1} and CO_{i+1}, and the bulky phenyl substituents decrease the rotational freedom of the peptide chains to such an extent that this Phe-Gly dipeptide isoster can ideally be applied for the development of conformationally constrained peptidomimetics.[4h]

In addition to the introduction of constraints in the peptide backbone, the turn-like structure induced by the DHP-2-one scaffold results in a constrained peptide that shows an excellent preorganization for macrocyclization. Currently we are investigating the use of this dipeptide isoster in the synthesis of constrained macrocyclic peptides. The incorporation of constrained elements in cyclic peptides has proven a useful method for further rigidification of the peptide, which often results in an improved receptor affinity and/or selectivity.[27] Also, these constrained derivatives proved to be important for SAR studies.

An especially attractive feature of the described synthetic approach is the highly modular character. In contrast to many existing Freidinger-type turn mimics, our MCR−alkylation−MCR strategy provides rapid access to tetra- and pentapeptidic turn mimics with possibilities for structural variation. It allows the rapid generation of diversely substituted dihydropyridones, via an initial MCR, to which a broad range of peptidic bromoacetamides can be attached by simple amide alkylation. Finally, a second peptide moiety is readily introduced by second MCR, such as the Ugi reaction, allowing additional diversification. This unique combination of complexity and diversity generation make this method ideally suitable for lead discovery and optimization.

Experimental Section

General Procedure I for the Ugi Reaction on Alkylated DHP-2-ones. To a solution of alkylated DHP-2-one **11** (0.22 mmol) in MeOH were subsequently added an aldehyde (0.33 mmol), an amine (0.33 mmol), and a carboxylic acid (0.24 and 0.22 mmol when 2,4-dimethoxybenzylamine is used[28]). The mixture was stirred at rt until the reaction was completed (determined by TLC). The resulting mixture was concentrated in vacuo and purified by column chromatography.

General Procedure II for the Passerini Reaction on Alkylated DHP-2-ones. To a solution of alkylated DHP-2-one **11** (0.22 mmol) in CH_2Cl_2 (367 μL) were added an aldehyde (0.33 mmol) and a carboxylic acid (0.24 mmol). The mixture was stirred at room temperature until the reaction was completed (determined by TLC). The resulting mixture was concentrated in vacuo and purified by column chromatography.

Alkylated DHP-2-one 11. To a solution of NaH (60 w%, 126 mg, 3.1 mmol) in dry DMF (20 mL) at 0 °C was added dropwise a solution of DHP-2-one **5a** (1.00 g, 2.9 mmol) in dry DMF (10 mL). After stirring for 75 min. at 0 °C, *tert*-butyl bromoacetate (0.51 mL, 3.4 mmol) was added. The mixture was stirred and slowly warmed to room temperature overnight, after which the reaction was concentrated in vacuo. The residue was dissolved in EtOAc (200 mL), washed with H_2O (2 × 150 mL) and brine (100 mL), and dried over $MgSO_4$. The crude product was purified by column chromatography (*c*-hexane/EtOAc 9:1 → 8:2) to afford **11** (1.26 g, 2.7 mmol, 93%) as a white foam. ^1H (250 MHz, $CDCl_3$): δ (ppm) 7.36−7.14 (m, 15H), 5.54 (d, J = 4.5 Hz, 1H), 4.40 (d, J_{AB} = 17.3 Hz 1H), 4.32 (d, J = 4.5 Hz, 1H), 3.96 (d, J_{AB} = 17.3 Hz 1H), 1.42 (s, 9H). ^{13}C NMR (63 MHz, $CDCl_3$): δ (ppm) 167.3 (C), 165.0 (C), 162.6 (C), 142.2 (C), 135.5 (C), 135.4 (C), 134.5 (C), 129.5 (2 CH), 129.4 (CH), 128.9 (3 CH), 128.5 (4 CH), 128.3 (CH), 128.1 (2 CH) 126.8 (2 CH), 111.2 (CH), 82.5 (C), 70.4 (C), 50.9 (CH), 47.8 (CH_2), 28.1 (3 CH_3). IR (KBr): 2977 (w), 2931 (w), 2360 (w), 2134 (m), 1741 (s), 1699 (s), 1372 (s), 1230 (s), 1153 (s), 759 (m), 687 (s). HRMS (EI, 70 eV): calcd for $C_{30}H_{28}N_2O_3$ (M^+) 464.2094, found 464.2090.

Ugi Product 12a. According to General Procedure I, reaction between alkylated DHP-2-one **11** (100 mg, 0.22 mmol), paraformaldehyde (10 mg, 0.33 mmol), benzylamine (36 μL, 0.33 mmol), and propionic acid (18 μL, 0.24 mmol) in MeOH (500 μL) afforded after 22 h **12a** (143 mg, 0.22 mmol, 100%) as a white foam. Column chromatography was performed with *c*-hexane/EtOAc 7:3 → 6:4. ^1H (400 MHz, DMSO, 403 K): δ (ppm) 7.80 (bs, 1H), 7.67−7.63 (m, 2H), 7.44−7.40 (m, 2H), 7.38−7.20 (m, 12H), 7.07−7.02 (m, 2H), 7.01−6.97 (m, 2H), 5.68 (d, J = 7.2 Hz, 1H), 5.21 (d, J = 7.2 Hz, 1H), 4.28 (d, J_{AB} = 15.7 Hz, 1H), 4.14 (d, J_{AB} = 15.7 Hz, 1H), 4.04 (d, J_{AB} = 17.1 Hz, 1H), 3.91 (d, J_{AB} = 17.1 Hz, 1H), 3.65 (s, 2H), 2.18−1.97 (m, 2H), 1.37 (s, 9 H), 0.95 (t, J = 7.4 Hz, 3H). ^{13}C NMR (101 MHz, DMSO, 403K): δ (ppm) 173.0 (C), 168.9 (C), 166.1 (C), 165.8 (C), 138.9 (C), 138.6 (C), 137.1 (C), 136.6 (C), 133.9 (C), 128.2 (2 CH), 127.9 (CH), 127.7 (2 CH), 127.7 (2 CH), 127.6 (2 CH), 126.9 (CH), 126.8 (4 CH), 126.6 (CH), 126.5 (4 CH), 126.3 (CH), 111.8 (CH), 80.9 (C), 63.1 (C), 49.4 (CH_2), 49.2 (CH_2), 46.6 (CH_2), 41.9 (CH), 27.0 (3 CH_3), 24.6 (CH_2), 8.3 (CH_3). IR (neat): 3362 (w), 2978 (w), 1742 (m), 1663 (s), 1495 (m), 1366 (m), 1225 (m), 1152 (s), 762 (m), 696 (s), 590 (m), 519 (m). HRMS (EI, 70 eV): calcd for $C_{41}H_{43}N_3O_5$ (M^+) 657.3197, found 657.3211.

Pentapeptide Mimic 19a. According to General Procedure II, reaction between alkylated DHP-2-one **18** (100 mg, 0.18 mmol), paraformaldehyde (8 mg, 0.27 mmol), benzylamine (30 μL, 0.27 mmol), and (*Z*)-Gly-OH (41 mg, 0.20 mmol) in MeOH/CH_2Cl_2 5:1 (1.2 mL)[29] afforded after 26 h **19a** (117 mg, 0.13 mmol, 72%) as a white foam. Column chromatography was performed with *c*-hexane/EtOAc 6:4 → 1:1. ^1H (400 MHz, DMSO, 403 K): δ (ppm) 7.84 (s, 1H), 7.74−7.66 (m, 3H), 7.56−7.53 (m, 2H), 7.38−7.22 (m, 22H), 7.08−7.03 (m, 2H), 6.99−6.96 (m, 2H), 6.57 (bs, 1H),

(27) Cheng, R. P.; Suich, D. J.; Cheng, H.; Roder, H.; DeGrado, W. F. *J. Am. Chem. Soc.* **2005**, *123*, 12710–12711, and references therein.

(28) Partial cleavage of the DMB group took place under acidic conditions, and therefore 1 equiv of acid was used in the reactions using 2,4-dimethoxybenzylamine.

(29) CH_2Cl_2 was added to increase the solubility of the dihydropyridone starting material, since it is very poorly soluble in MeOH.

5.60 (d, $J = 7.1$ Hz, 1H), 5.18 (d, $J = 7.1$ Hz, 1H), 5.15 (s, 2H), 5.07 (s, 2H), 4.25 (d, $J_{AB} = 15.7$ Hz, 1H), 4.18 (d, $J_{AB} = 15.7$ Hz, 1H), 4.18 (d, $J_{AB} = 19.3$ Hz, 1H), 3.90 (d, $J = 5.8$ Hz, 2H), 3.87 (d, $J_{AB} = 19.3$ Hz, 1H), 3.84−3.61 (m, 2H), 3.73 (d, $J_{AB} = 17.2$ Hz, 1H), 3.64 (d, $J_{AB} = 17.2$ Hz, 1H). ^{13}C NMR (101 MHz, DMSO, 403 K): δ (ppm) 168.7 (2 C), 168.5 (C), 166.8 (C), 165.4 (C), 155.4 (C), 139.2 (C), 138.9 (C), 137.2 (C), 136.6 (C), 136.0 (C), 135.4 (C), 134.1 (C), 128.5−126.4 (30 CH), 111.2 (CH), 65.3 (CH_2), 65.0 (CH_2), 63.3 (C), 49.3 (CH_2), 48.5 (CH_2), 46.5 (CH_2), 42.1 (CH), 41.5 (CH_2), 40.3 (CH_2). IR (neat): 3347 (w), 3063 (w), 2945 (w), 1719 (m), 1651 (s), 1495 (m), 1445 (m), 1387 (m), 1341 (m), 1244 (m), 1186 (s), 1179 (s), 1030 (w), 959 (w), 737 (m), 696 (s), 590 (w). HRMS (FAB): calcd for $C_{53}H_{50}N_5O_8$ (MH^+) 884.3654, found 884.3637.

Pentapeptide Mimic 19d. To a solution of **19b** (90 mg, 0.10 mmol) in CH_2Cl_2 (0.5 mL) was added TFA (0.5 mL). The mixture was stirred for 45 min at room temperature followed by removal of the solvent in vacuo and co-evaporation with toluene. The crude product was purified by column chromatography (EtOAc/*c*-hexane 7:3 → 8:2) to obtain **19d** (55 mg, 0.07 mmol, 70%) as a white foam.^{1}H (400 MHz, $CDCl_3$): δ (ppm) 7.68 (bs, 1H), 7.63 (d, $J = 7.2$ Hz, 2H), 7.40−7.18 (m, 21H), 7.02 (d, $J = 6.8$ Hz, 2H), 6.59 (bs, 1H), 6.34 (bs, 1H), 5.71 (bs, 1H), 5.65 (d, $J = 7.2$ H, 1H), 5.20 (d, $J = 6.8$ Hz, 1H), 5.14 (s, 2H), 5.10 (s, 2H), 4.01−3.87 (m, 4H), 3.80−3.57 (m, 4H). ^{13}C NMR (101 MHz, $CDCl_3$): δ (ppm) 170.4 (C), 169.5 (C), 169.0 (C), 167.4 (C), 167.0 (C), 156.6 (C), 140.7 (C), 138.4 (C), 136.7 (C), 136.3 (C), 135.3 (C), 134.4 (C), 129.1 (CH), 128.9 (4 CH), 128.8 (4 CH), 128.7 (3 CH), 128.5 (3 CH), 128.3 (3 CH), 128.2 (2 CH), 128.0 (3 CH), 127.3 (2 CH), 112.4 (CH), 67.3 (2 CH_2), 64.4 (C), 48.2 (CH_2), 44.3 (CH_2), 43.0 (CH_2), 42.2 (CH), 41.3 (CH_2). IR (neat): 3337 (w), 3063 (w), 1719 (m), 1655 (s), 1651 (s), 1497 (s), 1389 (m), 1240 (m), 1215 (m), 1190 (m), 1036 (w), 959 (w), 754 (s), 698 (s). HRMS (FAB): calcd for $C_{46}H_{44}N_5O_8$ (MH^+) 794.3184, found 794.3192.

Acknowledgment. This work was performed with financial support from the Dutch Science Foundation (NWO, VICI grant). Dr. H. Peeters (University of Amsterdam, The Netherlands) is kindly acknowledged for conducting HRMS measurements.

Supporting Information Available: Detailed experimental methods and characterization data (^{1}H and ^{13}C NMR, IR, HRMS) for all new compounds, details of the modeling studies, crystallographic data for **10** in CIF format, and data of the VT and DMSO titration NMR experiments. This material is available free of charge via the Internet at http://pubs.acs.org.

JO802052J